



**Solution-phase synthesized iron telluride nanostructures
with controllable thermally triggered p-type to n-type
transition**

Journal:	<i>Nanoscale</i>
Manuscript ID	NR-ART-08-2018-006418.R1
Article Type:	Paper
Date Submitted by the Author:	03-Oct-2018
Complete List of Authors:	Zheng, Wei; Iowa State University, Department of Chemical and Biological Engineering Hong, Sungbum; LG Company Min, Bokki; Iowa State University, Department of Chemical and Biological Engineering Wu, Yue; Iowa State University, Department of Chemical and Biological Engineering;





Journal Name

ARTICLE

Solution-phase synthesized iron telluride nanostructures with controllable thermally triggered p-type to n-type transition

Received 00th January 20xx,
Accepted 00th January 20xx

DOI: 10.1039/x0xx00000x

www.rsc.org/

Wei Zheng,^a Sungbum Hong,^b Bokki Min^a and Yue Wu^{*a}

The switchability of electrical property has recently attracted much attention due to their potential applications in memories, sensors, and resistive switches. Here, a solution-phase synthesis of iron telluride nanostructures with reversible and reproducible switching behavior between p- and n-type conduction is demonstrated by a simple change of temperature without crystal structure change. The transition temperature of FeTe₂ to switch from p-type to n-type is strongly dependent on the original ratio of precursors and sintering time. Further studies confirm the switching is derived from the valence change effect and a proof-of-concept thermally triggered p-n diode has been demonstrated.

Introduction

Materials with switchable physical properties have been attracting growing interest due to the potential applications in memories, sensors, and switches¹⁻⁴. For example, external stimuli such as light irradiation, electric field, temperature, and pressure can induce changes in their electronic, magnetic, optical and mechanical properties^{5,6}. Therefore, the ability to design and control the desired changes under external stimuli is the key prerequisite for the modern functional materials and devices.

Recently, numerous transition metal chalcogenides exhibiting switching electronic properties under temperature stimulus have been reported. Tom Nilges⁷ et al reported Ag₁₀Te₄Br₃ can switch its electrical properties by a simple change of temperature due to high silver mobility, a non-stoichiometric range, and an internal redox process. A reversible p-n-p type conduction switching property in AgCuS material caused by phase transition has been reported by Kanishka Biswas's group⁸. Thomas Palstra et al⁹ showed that the electrical property can be changed in marcasite FeSe_{2-δ} by effect of vacancies. However, the commercialization is hampered by low scalability^{10,11} and high cost of these materials. More importantly, it is difficult to precisely control the transition temperature intrigued by temperature.

Here, we show a low-cost and scalable solution-phase synthesis of FeTe₂ using a robust, one-pot approach at low temperature and atmospheric pressure. We also demonstrate that the switching temperature can be fine-tuned by changing the original precursor ratio. The vacancy concentration can be further controlled by changing the sintering time, which makes it possible to precisely adjust the switching temperature. Last but not least, a proof-of-concept thermally triggered p-n diode device has been developed based on the above results.

Results and discussion

The synthesis includes a two-step one-pot synthesis of the growth of Te nanowires and the conversion of Te nanowires into FeTe₂ shown in Fig 1a. The growth of Te nanowires is based on our previous reports¹²⁻¹⁴. The product of the large-scale synthesis of FeTe₂ is first analysed using X-ray diffraction (XRD). The result in Fig 1b show that the product of Fe:Te=1:2 original ratio (which is denoted as FeTe₂ in this paper) can be indexed as pure orthorhombic phase FeTe₂ (Red lines: JCPDS #14-0419). Fig 1c is the XRD pattern of Fe:Te=1:1 ratio (which is denoted as FeTe_{2-2x}Fe in this paper) and it can also be indexed as same pure orthorhombic phase FeTe₂.

^a Department of Chemical and Biological Engineering, Iowa State University, Ames, Iowa 50011, USA.

^b LG Company, Munji-ro 188, Yuseong-gu, Daejeon, South Korea, 34122

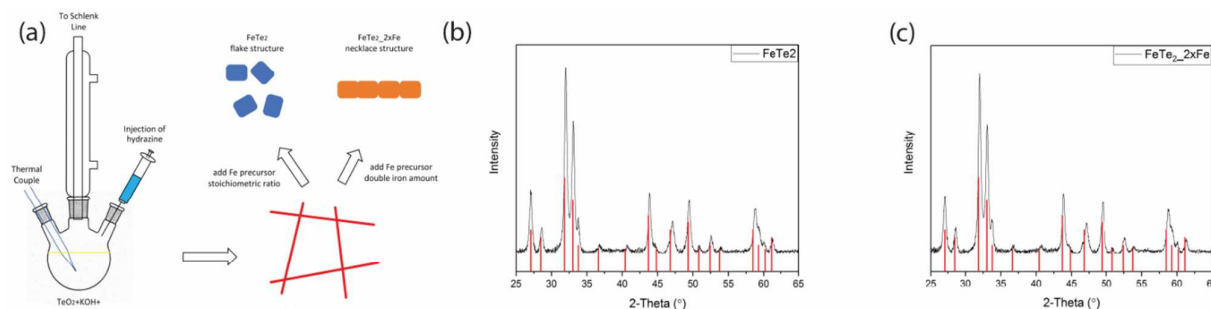


Figure 1 (a) Schematic illustration of the synthesis of FeTe₂ and FeTe₂_2xFe. (b) XRD patterns of FeTe₂ disk. (c) XRD patterns of FeTe₂_2xFe disk.

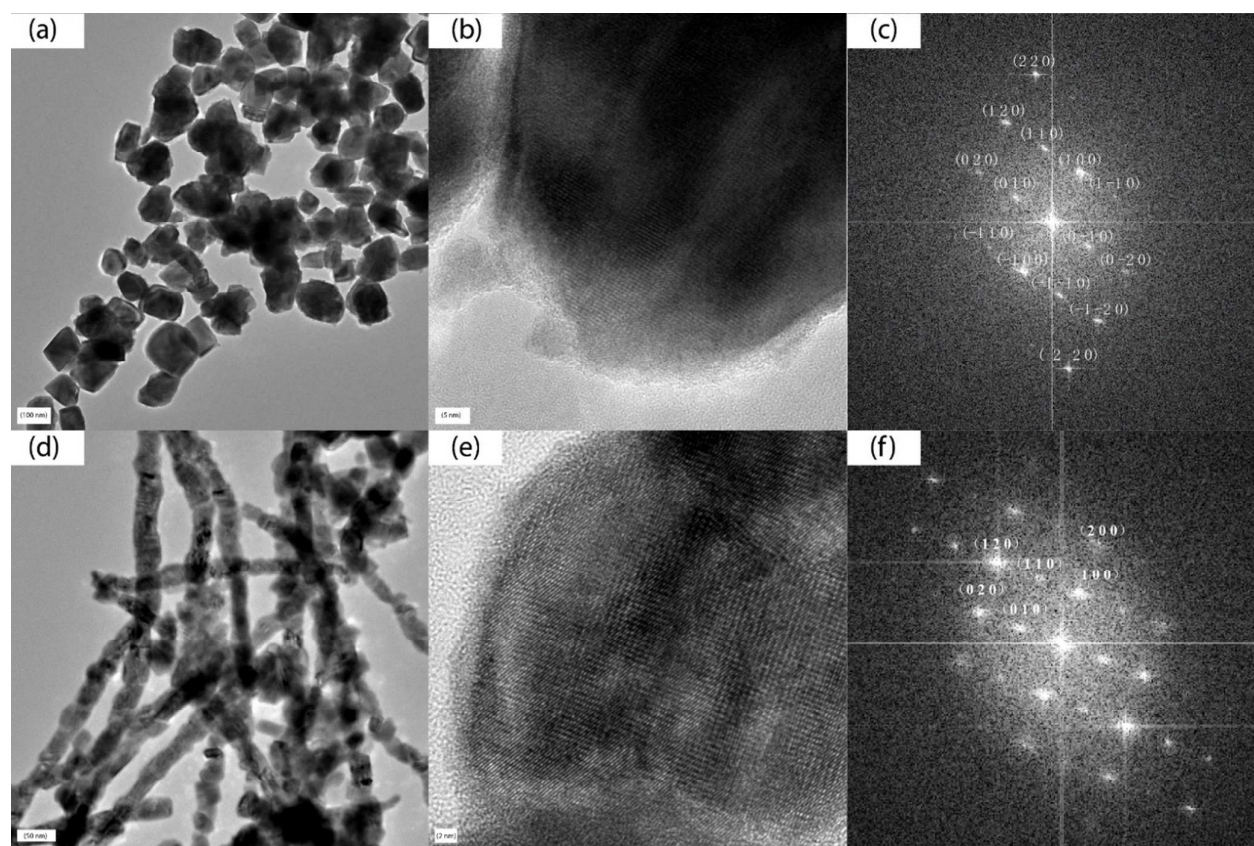


Figure 2 (a) TEM image of FeTe₂ (b) HRTEM image of FeTe₂ (c) FFT of Fig 2b (d) TEM image of FeTe₂_2xFe (e) HRTEM image of FeTe₂_2xFe (f) FFT of Fig 2e

The composition and morphology of our product are further verified by the transmission electron microscope (TEM) study. Fig 2a and 2d are the low-magnification TEM image of FeTe₂ and FeTe₂_2xFe, respectively. Notably, iron telluride morphology can be easily adjusted by the initial amount of iron precursor. FeTe₂ has flake structure while FeTe₂_2xFe

shows necklace structure. Fig 2b and Fig 2c are the high-resolution TEM (HRTEM) of FeTe₂ and its corresponding fast Fourier transform (FFT) image. HRTEM of FeTe₂_2xFe and its corresponding FFT image are shown in Fig 2e and Fig 2f. Both of FeTe₂ and FeTe₂_2xFe are further proved to be the same orthorhombic phase of FeTe₂ (space group is 58).

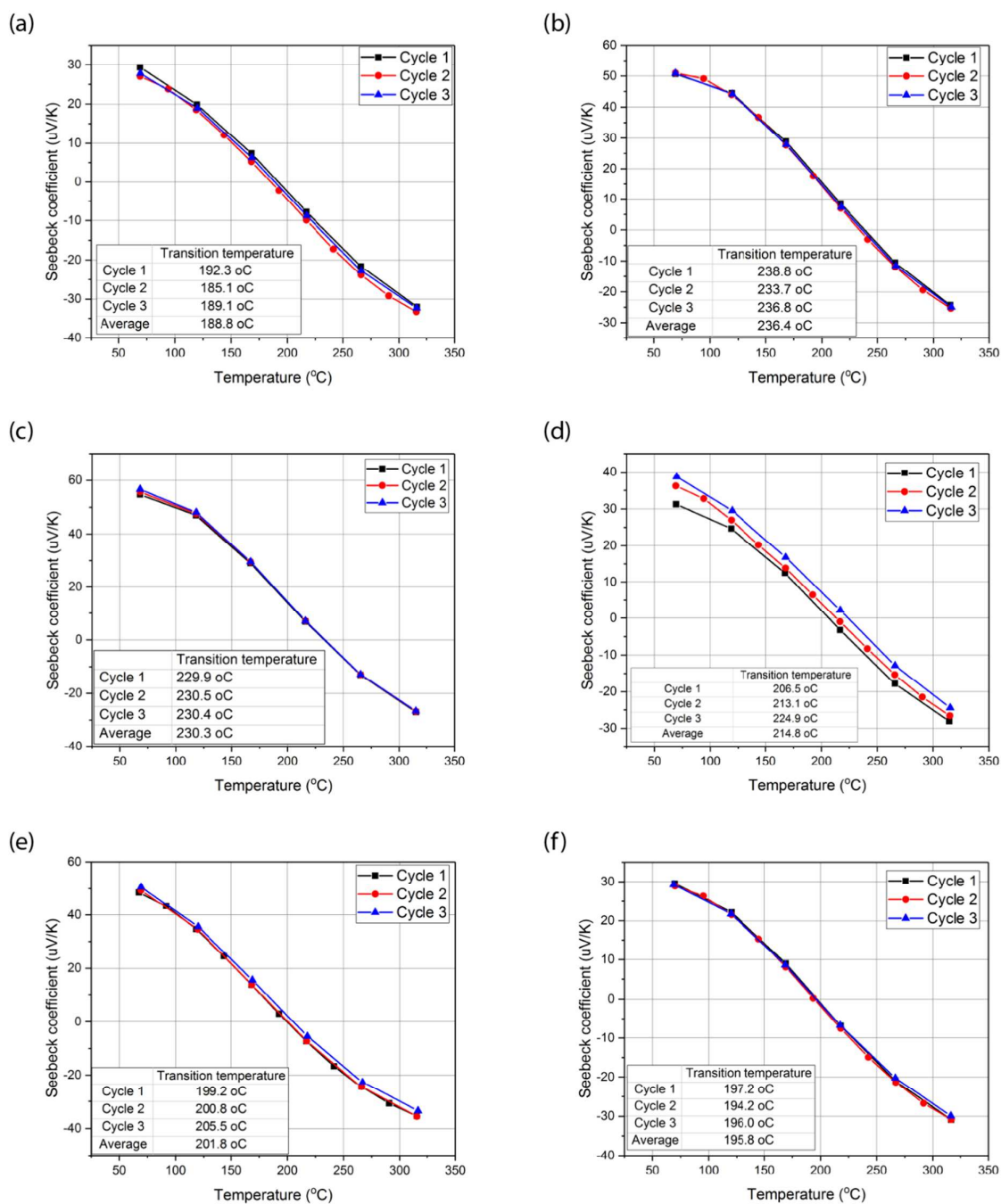


Figure 3 (a) Seebeck coefficient of FeTe₂_{2x}Fe (sintering time: 3 minutes) (b-f) Seebeck coefficient of FeTe₂ at different sintering time: (b) 3 minutes; (c) 6 minutes (d) 20 minutes (e) 30 minutes (f) 60 minutes.

In both syntheses, the only difference is the amount of the iron precursor, while all other experimental conditions remain the same, so we attribute the morphology change due to reaction kinetics¹⁵⁻¹⁷: with dilute iron precursor concentration (1:2 ratio), iron cations entering solid telluride from the solution is concentration controlled, so the new iron telluride phase (orthorhombic structure) segregates at the surface of tellurium phase (hexagonal structure)^{12, 14}. Strong structure

stress breaks down the tellurium nanowires, ultimately forming flake structures. While in the higher iron precursor concentration case (double iron precursor), the large availability of iron precursor accelerates the diffusion into the tellurium nanowires, so iron telluride can be rapidly converted at both the surface and interior of tellurium nanowires, and the wire structure can be conserved while forming the necklace structure to release the stress.

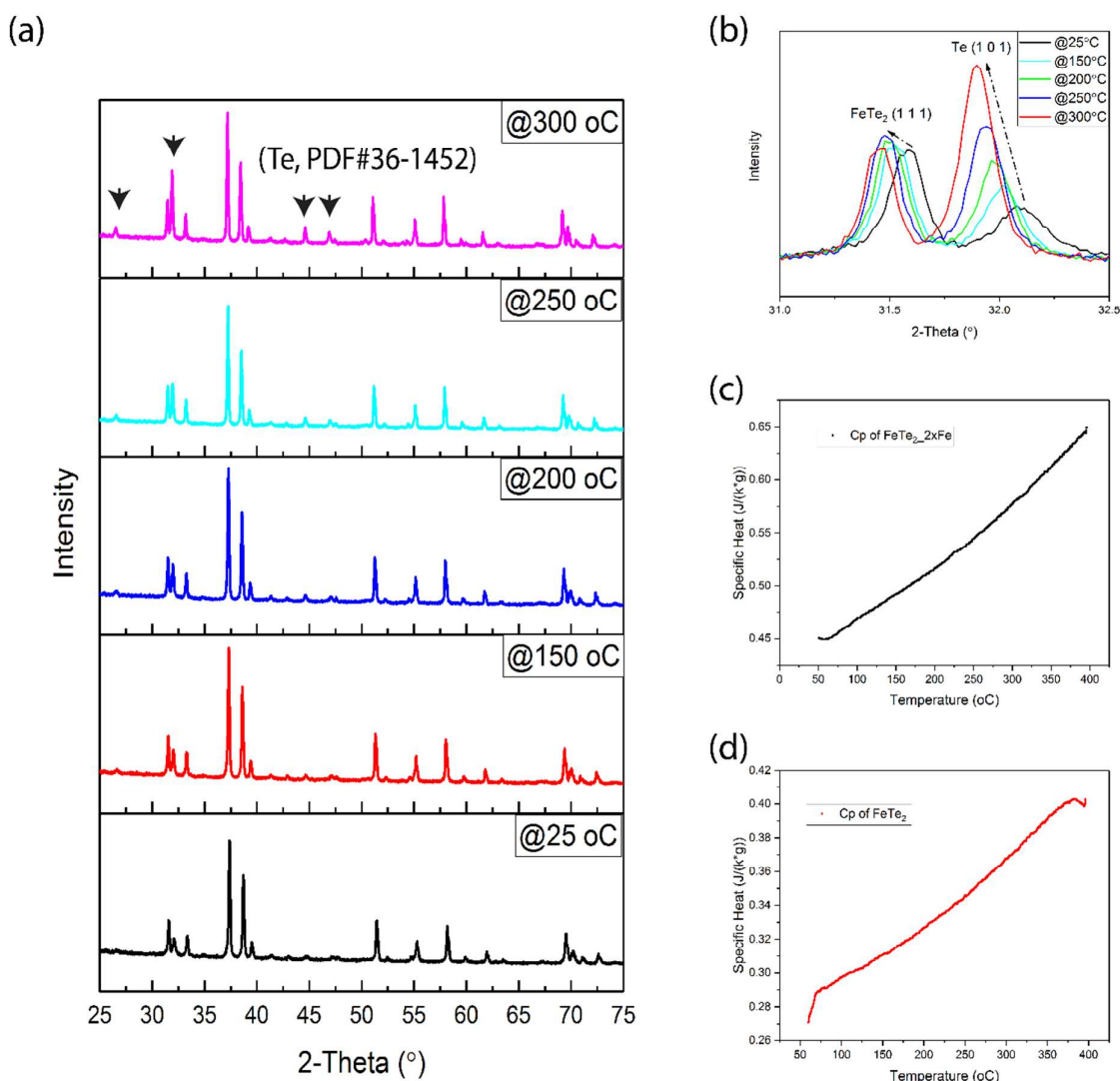


Figure 4 In-situ XRD of FeTe₂ disk sample 2-Theta from 25 to 75-degree (b) In-situ XRD of FeTe₂ disk sample 2-Theta from 31.0 to 32.5 degree (c) DSC result of FeTe₂_{2XFe} (d) DSC result of FeTe₂

Journal Name

ARTICLE

We further scale up the reaction to 1 liter-sized reactor and high yield (> 4 g per batch) is achieved, which enables us to sinter several FeTe₂ disks with 1 cm diameter by Spark Plasma Sintering (SPS) and investigate their electrical and thermal properties. The Seebeck coefficient of FeTe_{2-x}Fe has been measured from 70 °C to 320 °C and is shown in Fig 3a. The Seebeck coefficient decreases monotonically with increasing temperature and switches from positive value (p-type) to negative value (n-type). Every sample has been tested three times and this switching phenomenon is highly reproducible and reversible. The actual transition temperature for every cycle is recorded by our Linseis LSR-3 system and the calculated average transition temperature values are summarized in the insert table in Fig 3a. Fig 3b is the Seebeck coefficient of FeTe₂ and it also shows similar reproducible and reversible switching behaviour. Compared to FeTe_{2-x}Fe, FeTe₂ has a higher positive Seebeck coefficient value below 188.8 °C. The average transition temperature from p-type to n-type is 236.43 °C for FeTe₂ while is 188.8 °C for FeTe_{2-x}Fe. Between 188.8 °C and 236.43 °C, FeTe₂ shows p-type behaviour and FeTe_{2-x}Fe already turns to n-type material. Both of FeTe₂ and FeTe_{2-x}Fe switch to n-type when the temperature is above 236.43 °C while the absolute Seebeck coefficient value of FeTe₂ is smaller than FeTe_{2-x}Fe.

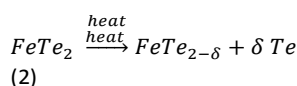
In order to understand this interesting p to n transition, a series of investigations have been performed. In most cases, such a transition could result from either crystal structural change or the vacancy concentration change. To check the possibility of crystal structure change, in-situ XRD has been performed and the results are shown in Fig 4a and 4b. The FeTe₂ sample is sealed in a heating sample holder with Argon gas protection. The volume of unit cell will expand when temperature is rising (d increase), which means the 2-theta will be decreased according to $2d\sin\theta=\lambda$ equation. As we can see from Fig 4b, both FeTe₂ peak and Te peak shift left during temperature rising. The peak intensity will also increase when temperature increases¹⁸. However, compared to FeTe₂ peak (1 1 1), tellurium peak (1 0 1) (JCPDS #36-1452) start to emerge and get stronger with increasing temperature. The differential scanning calorimetry (DSC) study further confirms the lack of crystal structure change in FeTe_{2-x}Fe (shown in Fig 4c) and FeTe₂ (shown in Fig 4d), as neither of which shows any peak in the temperature range from 70 °C to 350 °C, which indicates the lack of phase change during this temperature range.

As suggested from Fig. 4a and 4b where Te peaks appear and strengthen with increasing temperature, the Te vacancy-induced p to n transition is more plausible. Indeed, the electrical transport of matter in solid phase is directly dependent upon deviations from ideal crystalline order¹⁹. For

transition metal chalcogenide, it will show p-type behaviour when there is excess chalcogen while show n-type behaviour when there is a deficiency in chalcogen⁴. In our case, during the temperature increase, isolated tellurium from iron telluride nanostructures will form polytelluride and the system has more tellurium vacancy defects, which will change the electrical conductivity from p-type to n-type. This explanation can be expressed in equation (1) with Kröger symbolism.



The subscript means the lattice site while the superscript corresponds to the electric charge of the relative to the site. The body indicates the species. According to electronegativity, iron will have positive charge while tellurium keeps negative charge. On the left of equation (1), one tellurium anion is sitting on a tellurium lattice site with negative charge. During heating, it will decompose into one vacancy in the tellurium lattice site with negative charge while tellurium atom is in the interstitial site with neutrality charge. The Fermi energy will be changed because of the tiny change in volume of crystal during the formation of vacancy and because of the scattering of the electron waves at the defects¹⁹. Therefore, an increasing of tellurium vacancies will affect the valence state and change the electrical conductivity type. From macroscopic view, the equation can be written as following:



where δ represents a very small value that won't affect the crystal structure. Every sample has reproducible and reversible result, which means the process described by the equations (1) and (2) are truly reversible during cooling down.

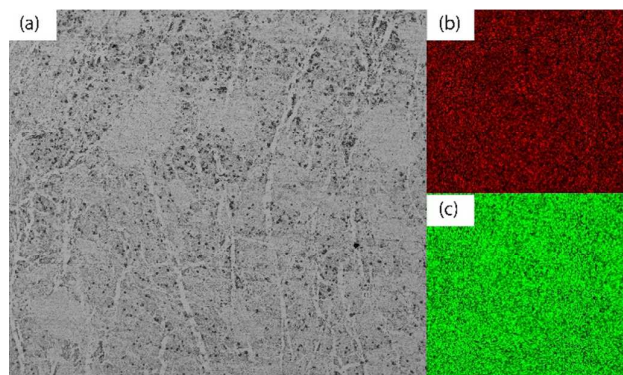
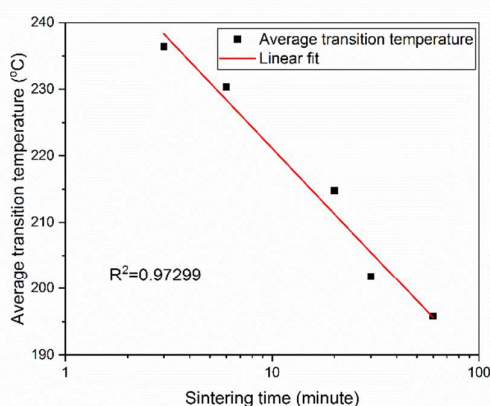


Figure 5 SEM EDS mapping results of FeTe₂ disk (FeTe₂@60 mins) (a) SEM image of FeTe₂ disk, magnification is 100x (b) Fe element mapping result (red colour) (c) Te element mapping result (green colour)

The Seebeck coefficient of FeTe₂ with different sintering times are also showed in Fig 3c (6 minutes; FeTe₂@6 mins), Fig 3d (20 minutes; FeTe₂@20 mins), Fig 3e (30 minutes; FeTe₂@30 mins), and Fig 3f (60 minutes; FeTe₂@60mins). Compared to Fig 3b which is sintered for 3 minutes (FeTe₂@3 mins), FeTe₂@6 mins, FeTe₂@20 mins, FeTe₂@30 mins and FeTe₂@60 mins disks show obvious drop in the transition temperature. All the disks have been tested 3 times and all showed reproducible and reversible switch behaviour. As shown in Fig 5, the energy-dispersive X-ray (EDX) analysis of the sintered FeTe₂@60 mins disk indicates that there are only Fe and Te elements in this disk. The atomic ratio of Fe and Te with different sintering times are showed in table 1. All the sinterings are conducted at 600 °C while the melting point of pure Tellurium is 445 °C²⁰. Therefore, equation 2 becomes non-reversible at the sintering process due to the vaporization of tellurium. As seen from table 1, the Te amount decrease when sintering time is increased. The average transition temperature for FeTe₂@6 mins, FeTe₂@20 mins, FeTe₂@30 mins and FeTe₂@60 mins switch from p-type to n-type are 230.27 °C, 214.8 °C, 201.8 °C and 195.8 °C. Fig 6 is the plot of the average transition temperature v.s. the logarithm of sintering time. There is a linear relationship between average transition temperature and logarithm of sintering time. The longer the sintering time, the lower the transition temperature.

Table 1 SEM EDS mapping results of FeTe₂ disks with different sintering times

Sample	Atomic Ratio	Fe	Te
FeTe ₂ @3 mins		32.07	67.93
FeTe ₂ @6 mins		32.41	67.59
FeTe ₂ @20 mins		32.60	67.40
FeTe ₂ @30 mins		33.26	66.74
FeTe ₂ @60 mins		33.73	66.27

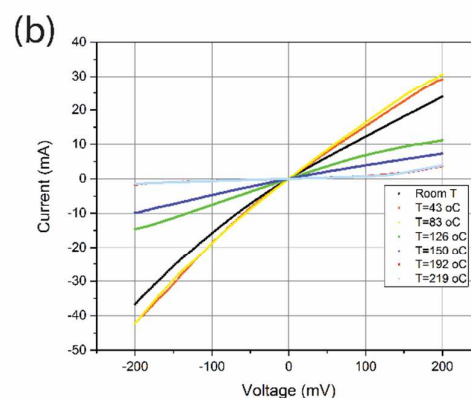
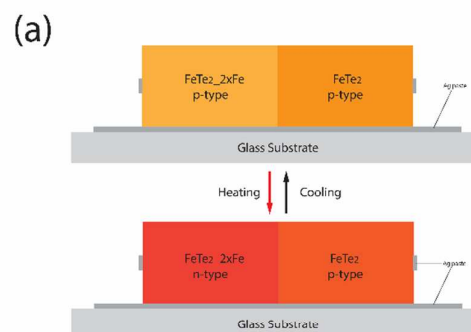
Figure 6 Average transition temperature of FeTe₂ v.s. logarithm of sintering time

In principle, the concentration of tellurium vacancies can be calculated by the laws of dilute solution as the concentration of tellurium vacancies is very small compared to

the total amount of Te atoms^{19, 21}. The reaction rate and sample thickness can be assumed to be constant²²⁻²⁴, the concentration of tellurium vacancies model can be expressed as following:

$$(C_t - C_{t=0}) / (C_{\infty} - C_{t=0}) = 1 - \exp(-kt/L) \quad (3)$$

where t is the sintering time, k is the reaction rate, and L is the sample thickness. C_t is the concentration of tellurium vacancies at time t . This equation explains the linear relationship between vacancy concentration and logarithm of sintering time. The vacancy concentration does directly impact the carrier type and concentration as there will be more tellurium vacancies when the sintering time increases, so the transition temperature will decrease as a result. To the best of our knowledge, it has always been challenging to tune the transition temperature in a large temperature window. However, for our FeTe₂ system, the transition temperature can be adjusted from 195.8 °C (FeTe₂@60 min) to 236.43 °C (FeTe₂@3 min). More importantly, the transition temperature has a linear relationship with the logarithm of sintering time. In other words, the transition temperature can be fine-tuned by simply changing the sintering time, which makes its switching behaviour more controllable and useful.

Figure 7 (a) Schematic illustration of thermally triggered p-n diode device (b) I-V curve of FeTe₂-FeTe₂-2xFe

To demonstrate potential device applications, a proof-of-concept thermally-triggered p-n diode device has been

constructed. The device is schematically shown in Fig 7a. Same amounts of FeTe₂ powder and FeTe_{2-2x}Fe powder are loaded into one graphite die and sintered together by SPS. Then the bilayer disk is diced and fixed on the glass with electrical connection. Then it is placed on top of a heating source with the I-V curves recorded at different temperature (shown in Fig 7b). Below the transition temperature of FeTe_{2-2x}Fe, both FeTe₂ and FeTe_{2-2x}Fe are p-type and the I-V curves are straight lines (ohmic contact). The I-V curve will immediately show p-n diode behaviour when the temperature is higher than the transition temperature of FeTe_{2-2x}Fe (T₁) while lower than the transition temperature of FeTe₂ (T₂). This thermally triggered p-n diode behaviour is fully reversible and reproducible. More importantly, it is made from the same crystalline structure of FeTe₂ and FeTe_{2-2x}Fe, which has no structure mismatch stress induced by thermal expansion.

Experimental details

Tellurium oxide (TeO₂, 99.99%) was purchased from Alfa Aesar. Polyvinylpyrrolidone (PVP, average 40,000 g/mol), potassium hydroxide (KOH, 99.99%), hydrazine (anhydrous, 98%), and iron chloride (FeCl₃, 97%) were purchased from Sigma-Aldrich. Hydrazine monohydrate (79%) was purchased from Tokyo Chemical Industry and Ethylene glycol (EG) was purchased from VWR.

For the synthesis of FeTe₂, 5.145 g TeO₂ (32.25 mmol), 14.625 g of KOH, and 450 ml of EG were added to 1 L three-neck flask with magnetic stirring initiated for continuous mixing. The reactor was heated to 70 °C and 9 g of PVP was added to the flask slowly. Then, the temperature was raised to 110 °C and 5.5 ml of hydrazine was rapidly injected into the reactor. The temperature was maintained at 110 °C for 1 hour under nitrogen gas protection. As the Te nanowires growing, an iron precursor solution was made in a nitrogen-filled glovebox. 2.6153 g of FeCl₃, and 50 ml of EG were added to a 100-ml beaker and heated to 80 °C. 26 ml hydrazine was slowly added. After 1-hour reaction for Te nanowires growth, the temperature was set to 120 °C. When the temperature reaches 120 °C, all the iron precursor was rapidly injected. 4 hours after iron precursor injection, the reaction was stopped and cooled down naturally to room temperature. For the synthesis of FeTe_{2-2x}Fe, the only difference was that the amount of FeCl₃ was double to 5.2306 g.

Then, the as-synthesized FeTe₂ were washed three times with deionized (DI) water. The sediment after water washing was then soaked into hydrazine hydrate (30% volume ratio) and ethanol solvent. The soaking procedure was also protected by nitrogen gas and stirred by a magnetic bar. The mixture was then centrifuged three times by ethanol and the supernatant was discarded. The material was then dried overnight in the vacuum chamber at room temperature and brought directly into a nitrogen-filled glovebox for grinding with a mortar and pestle.

Conclusions

In summary, we have developed a large-scale solution-phase method to synthesize FeTe₂ nanostructures at low temperature and ambient pressure. The transition temperature can be adjusted by changing the amount of iron precursor. Notably, the transition temperature has a linear relationship with the logarithm of sintering time, making it precisely tuneable by controlling the sintering time. The in-situ XRD and DSC experiments showed the reason for switching is more likely due to the valence change effect caused by tellurium deficiency. The successful demonstration of thermally triggered p-n diode device indicates its potential application as thermal sensors or thermal resistors.

Conflicts of interest

There are no conflicts to declare

Acknowledgements

W. Z., S.H., B.M., and Y.W. gratefully thank for support from the Office of Naval Research (Award Number n00014-16-1-2066).

Notes and references

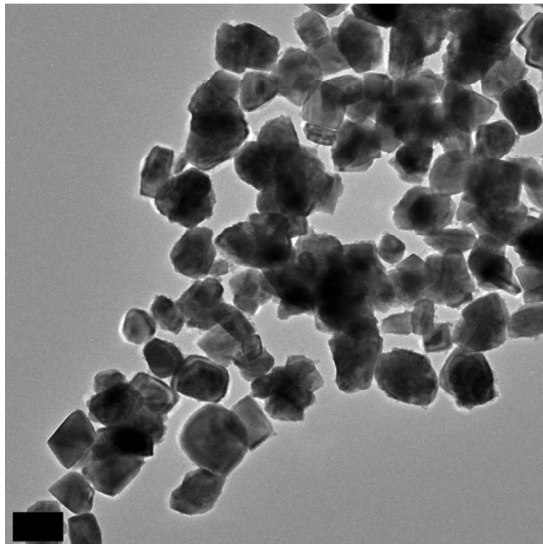
1. Y. V. Pershin and M. Di Ventra, *Advances in Physics*, 2011, **60**, 145-227.
2. R. Waser and M. Aono, *Nature materials*, 2007, **6**, 833-840.
3. R. Waser, R. Dittmann, G. Staikov and K. Szot, *Advanced materials*, 2009, **21**, 2632-2663.
4. J. J. Yang, D. B. Strukov and D. R. Stewart, *Nature nanotechnology*, 2013, **8**, 13-24.
5. O. Sato, *Nature chemistry*, 2016, **8**, 644-656.
6. W. Zhou, W. Zhao, Z. Lu, J. Zhu, S. Fan, J. Ma, H. H. Hng and Q. Yan, *Nanoscale*, 2012, **4**, 3926-3931.
7. T. Nilges, S. Lange, M. Bawohl, J. M. Deckwart, M. Janssen, H.-D. Wiemhöfer, R. Decourt, B. Chevalier, J. Vannahme and H. Eckert, *Nature materials*, 2009, **8**, 101-108.
8. S. N. Guin, J. Pan, A. Bhowmik, D. Sanyal, U. V. Waghmare and K. Biswas, *Journal of the American Chemical Society*, 2014, **136**, 12712-12720.
9. G. Li, B. Zhang, J. Rao, D. Herranz Gonzalez, G. R. Blake, R. A. de Groot and T. T. Palstra, *Chemistry of Materials*, 2015, **27**, 8220-8229.
10. E. Bastola, K. P. Bhandari, A. J. Matthews, N. Shrestha and R. J. Ellingson, *RSC Advances*, 2016, **6**, 69708-69714.
11. K. D. Oyler, X. Ke, I. T. Sines, P. Schiffer and R. E. Schaak, *Chemistry of Materials*, 2009, **21**, 3655-3661.
12. S. W. Finefrock, H. Fang, H. Yang, H. Darsono and Y. Wu, *Nanoscale*, 2014, **6**, 7872-7876.
13. H. Yang, J.-H. Bahk, T. Day, A. M. Mohammed, B. Min, G. J. Snyder, A. Shakouri and Y. Wu, *Nano letters*, 2014, **14**, 5398-5404.
14. W. Zheng, B. Xu, L. Zhou, Y. Zhou, H. Zheng, C. Sun, E. Shi, T. D. Fink and Y. Wu, *Nano Research*, 2017, 1-12.

ARTICLE

Journal Name

15. Y. Yan, J. S. Du, K. D. Gilroy, D. Yang, Y. Xia and H. Zhang, *Advanced Materials*, 2017.
16. X. W. Lou, Y. Wang, C. Yuan, J. Y. Lee and L. A. Archer, *Advanced Materials*, 2006, **18**, 2325-2329.
17. S. Fischer, J. K. Swabeck and A. P. Alivisatos, *Journal of the American Chemical Society*, 2017, **139**, 12325-12332.
18. Y. Waseda, E. Matsubara and K. Shinoda, *X-ray diffraction crystallography: introduction, examples and solved problems*, Springer Science & Business Media, 2011.
19. H. Schmalzried, *Solid state reactions*, Vch Pub, 1981.
20. A. Epstein, H. Fritzsche and K. Lark-Horovitz, *Physical Review*, 1957, **107**, 412.
21. R. Merkle and J. Maier, *Angewandte Chemie International Edition*, 2008, **47**, 3874-3894.
22. J. Maier, *Solid State Ionics*, 1998, **112**, 197-228.
23. G. M. CHOI and H. L. Tuller, *Journal of the American Ceramic Society*, 1988, **71**, 201-205.
24. M. Leonhardt, R. De Souza, J. Claus and J. Maier, *Journal of The Electrochemical Society*, 2002, **149**, J19-J26.

We report the solution-phase synthesis of iron telluride with controllable reversible switching behavior between



p- and n-type conduction.

